Power Conversion System Model and Control for Energy Stationary Storage

M. Andriollo, R. Benato, S. Dambone Sessa, F. Nucci, F. Siviero
Department of Industrial Engineering
University of Padova
Padova, Italy

F. Palone, M. Rebolini
Terna
Rome, Italy

***Abstract*—The paper describes the instantaneous control technique of a two stage Power Conversion System interfaced to an energy storage equipment. The control aims at regulating the active and reactive power exchange between the grid and the converter during the battery discharge and charge operations. The results of the control implementation in a Simulink® model of the Power Conversion System are compared with experimental measurements carried out by the Italian TSO Terna during an energy storage system power inversion.**

Keywords—power conversion system; energy storage systems; larege scale storage.

I INTRODUCTION

The two-stage DC/DC-DC/AC power conversion system (PCS) architecture is widely used to interface electrical energy electrochemical storage systems (ESS) with the high voltage network [1,2]. The ESS-connected DC-DC converter avoids the DC/AC stage overrating benefitting from the DC-bus voltage stabilization. In fact, a $\Delta u\%$ percentage DC-bus voltage variation with respect to the rated value due to the battery voltage fluctuations would result in an overrating of $1 + \Delta u\%$ for both the voltage and the current (maximum current corresponding to minimum battery voltage) and a consequent inverter power oversizing by $\approx 1 + 2\Delta u\%$. For instance, by assuming that battery voltage may vary by 20%, the inverter should be sized for the power:

$$P = V_{max} I_{max} = 1.2\, V_n \cdot 1.2\, I_n \approx 1.4\, P_n = P_n + \Delta P$$

with an inverter oversizing $\Delta P \approx 40\% P_n$. A two-stage PCS is therefore preferable even if a single-stage PCS could be practicable in principle. The paper presents the implementation in the Simulink® environment of the PCS control strategy, aimed at supply the instantaneous values of active and reactive power required by the electrical network. The promptness of the control strategy is verified, evaluating the delay between the input PCS command to switch ESS from charge to discharge mode for a predefined power value, and the moment when such value is reached within a ± 3% tolerance. According to the Italian Transmission System Operator (TSO) Terna prescriptions, such delay – called "time to phase inversion" must be lower than 300 ms.

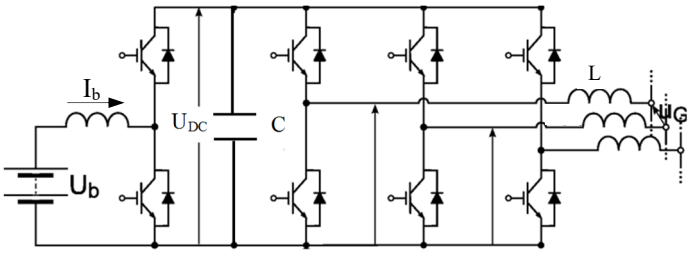

Fig. 1 Two-stage converter scheme

II PCS AND ESS CONTROL

From a control point of view, according to the electrical scheme of fig. 1, the DC voltage U_{DC} can be controlled only indirectly by regulating the grid current. In fact, the direct control of the DC-bus voltage by the inverter average switching functions has divergent zero dynamics, so corresponding operation would be unstable [3].

Hence, the ESS active power flow is managed by the DC/DC converter stage for both the discharge and charge operations, whereas the DC/AC converter stage controls the DC-bus voltage U_{DC} and the reactive power flow exchanged with the grid.

A. ESS Control

The DC/DC conversion stage controls the ESS supplied power, in order to obtain the reference active power P^* required from the grid. This control can be implemented by comparing the actual ESS current I_b with the reference value $I_b^* = P^*/U_b$.

The current error $\varepsilon_{I_b} = I_b^* - I_b$, conditioned by means of a PID block, can be used as a modulating signal of a PWM control for a non isolated bidirectional DC/DC converter. It is operated in the boost mode when battery is discharging or in the buck mode when battery is recharging. The block scheme of the ESS control, corresponding to the Matlab-Simulink® implementation, is shown in Fig. 2. The simulation results of the ESS power control shown in fig. 3 confirm the effectiveness of the control strategy.

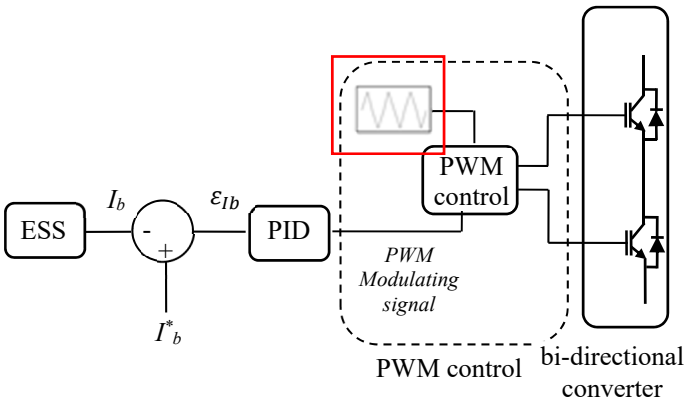

Fig. 2 ESS active power control

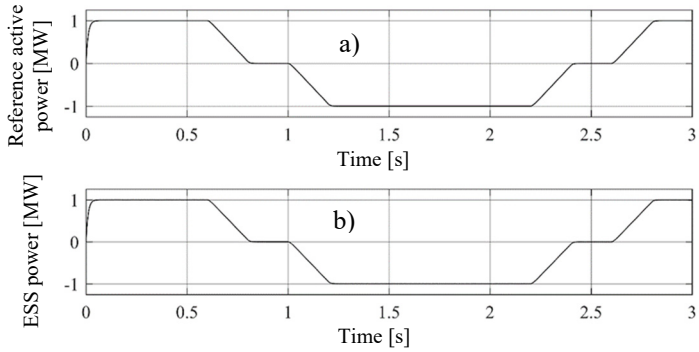

Fig. 3 a) Reference active power b) active power supplied by the battery

B. DC-Bus Voltage Control

By assuming a balanced three-phase system, the instantaneous input–output power balance between the grid and the power converter is given by:

$$i_b u_{DC} - u_{DC} C \frac{du_{DC}}{dt} = \sum_{k=1}^{3} e_{gk} i_{gk} \qquad (1)$$

where

k=1, 2, 3 phase index;
i_b=battery current;
i_{gk}=phase current;
e_{gk}=phase voltage;
C=DC bus capacitance.

In a synchronous rotating dq frame under a no-loss condition and by means of small signal linearization, from (1) it is possible to infer the dependence of the DC voltage U_{DC} on the inverter current direct component I_d is represented by the following transfer function [2]

$$\frac{\hat{u}_{dc}}{\hat{i}_d} = \frac{\sqrt{3}}{2} \frac{R_o}{(1 - R_o C s)} \qquad (2)$$

where:

R_0=U_{DC}/I_b is the steady state DC bus equivalent resistance;

$\hat{i}_d$ is the small-signal current related to the current direct component I_d which causes the corresponding variation of the-small-signal voltage $\hat{u}_{DC}$ related to U_{DC}.

Therefore, the voltage U_{DC} can be controlled by varying the active power P which the inverter exchanges with the grid with respect to the active power P_{ESS} supplied by the ESS. The current direct component $I'_{d_{inv}}$ corresponding to the inverter power P is:

$$I'_{d_{inv}} = P/\left(\sqrt{3}\, U_{grid}\right)$$

hence, this control strategy can be implemented by subtracting from the current direct component $I^*_{d\_inv}$ related to the active power P^* required from the grid, the current i_d, in order to obtain the inverter reference current direct component $I'^*_{d\_inv}$. Therefore, part of the power supplied by the ESS is used to charge the capacitor C, in order to reach the DC-bus reference voltage. When the DC-bus voltage U_{DC} reaches the reference value U^*_{DC} it implies that I'_{d_inv}=$I'^*_{d\_inv}$, as it is described in the block scheme of fig. 4. The reference current $I'^*_{d\_inv}$ is compared with the inverter actual current I_{d_inv}, in order to regulate the current direct component that the inverter exchanges with the grid and which is used to generate the inverter reference voltage $U^*_{inv.}$

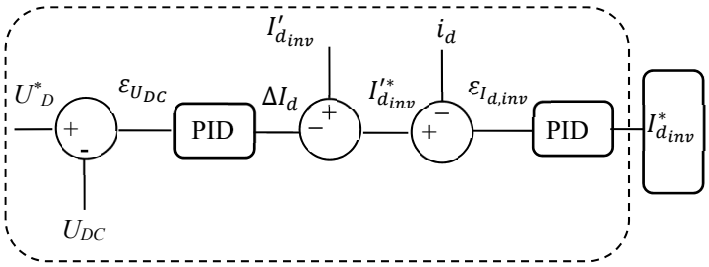

U_{DC} control

Fig. 4 DC bus voltage control

C. DC/AC Conversion Stage Control

The inverter voltage equations in the usual d,q frame can be written as:

$$U_{d_{inv}} = U_g - \omega L i_q + L \frac{di_d}{dt} \qquad (3)$$

$$U_{q_{inv}} = \omega L i_d + L \frac{di_q}{dt} \qquad (4)$$

where:

$U_{d_{inv}}$ and $U_{q_{inv}}$ are the inverter voltage direct and quadrature components;

U_g are the grid voltage direct and quadrature components.

Preliminary reference values of inverter voltage components $U^{I*}_{d_{inv}}$, $U^{I*}_{q_{inv}}$ can be obtained assuming steady state operation with reference values of the reactive power Q^* and the inverter

current d-component $I^*_{d_{inv}}$ (defined by the DC-bus voltage control):

$$U'^*_{q_{inv}} = \omega L I^*_{d_{inv}}$$

$$Q^* = \frac{3}{2} U_g I^*_{q_{inv}} = \frac{3}{2} \cdot \frac{U_g \left(U'^*_{d_{inv}} - U_g \right)}{\omega L} \Rightarrow$$

$$\Rightarrow U'^*_{d_{inv}} = U_g + \frac{2}{3} \cdot \frac{\omega L Q^*}{U_g}$$

Errors on current direct and quadrature components with respect to the reference values can be compensated by voltage corrections having opposite sign with respect to the corresponding current derivative, obtained from (3) and (4). By assuming to adopt a PI regulator, the following correction terms are introduced:

$$\Delta U_d = -k_p (i_{d_{inv}} - i^*_{d_{inv}}) - k_i \int (i_{d_{inv}} - i^*_{d_{inv}}) dt$$

$$\Delta U_q = -k_p (i_{q_{inv}} - i^*_{q_{inv}}) - k_i \int (i_{q_{inv}} - i^*_{q_{inv}}) dt$$

Fig. 5 shows the block scheme to obtain the instantaneous $U^*_{q_{inv}}$ and $U^*_{d_{inv}}$ values.

Once defined the inverter reference complex voltage as:

$$U^*_{d,q_{inv}} = U^*_{d_{inv}} + j \cdot U^*_{q_{inv}}$$

it is possible to infer the three inverter reference phase voltages $U^*_{inv,a}, U^*_{inv,b}, U^*_{inv,c}$ by passing from the d,q frame to the a, b, c one [4, 5].

The above described control strategy has been implemented in a Matlab Simulink model to drive, by means of a plain PWM technique, a three phase inverter connected to an ideal grid via three loss-less reactors. Fig 6 shows the full Simulink PCS model with the three PCS control subsystems.

The grid has been represented by means of a balanced three phase source. The outputs of the ESS control block consist on the command pulses for the buck-boost converter, whereas the cascade of the DC bus voltage control block and the inverter voltage generation ones generate the pulses to pilot the DC/AC conversion stage.

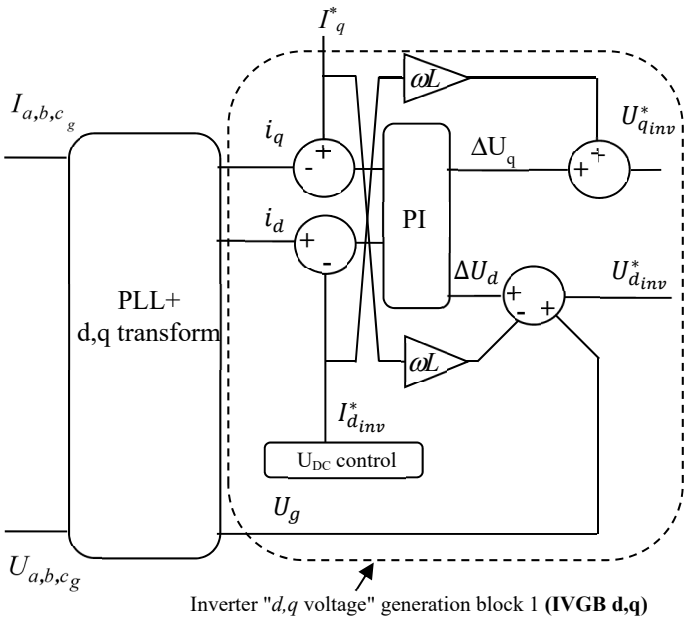

Inverter "d,q voltage" generation block 1 **(IVGB d,q)**

Fig. 5 Block scheme to obtain the instantaneous $U^*_{q\_inv}$ and $U^*_{d\_inv}$ values

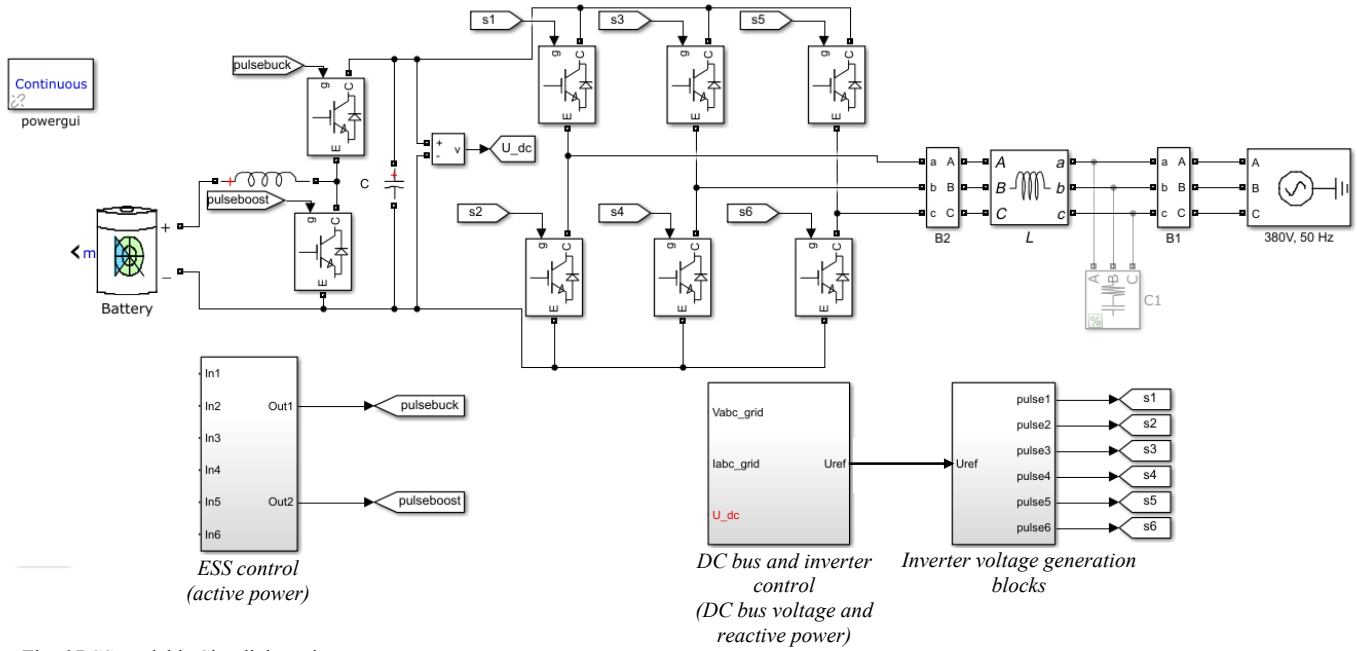

Fig. 6 PCS model in Simulink environment

III SIMULATION RESULTS

The power exchanged between the PCS and the grid has been compared with the power references for different cases. At first, a real Italian stationary storage installation, located in Flumeri, Campania, has been represented by means of the present PCS model and control. In this plant, two 1.2 MW Sodium-Sulphur (NaS) storage units [6-8] are connected to the grid by means of four two-stage converters (see fig. 7). A phase inversion from the storage unit discharge mode to the charge one has been simulated by varying the grid required active power from +2.4 MW to -2.4 MW.

The model results have been compared with experimental measurements carried out by Terna during the same power inversion in the real above mentioned storage installation. It is worth noting that the EES has been modelled by means of a standard Matlab Simulink battery block, because of the lack of detailed information about the characteristics of the batteries used in the real installation.

In fig. 8 and 9 two power variation times have been hypothesized, equal to 10 ms and 30 ms, since the actual dynamic behaviour and management of the batteries during the test are unknown.

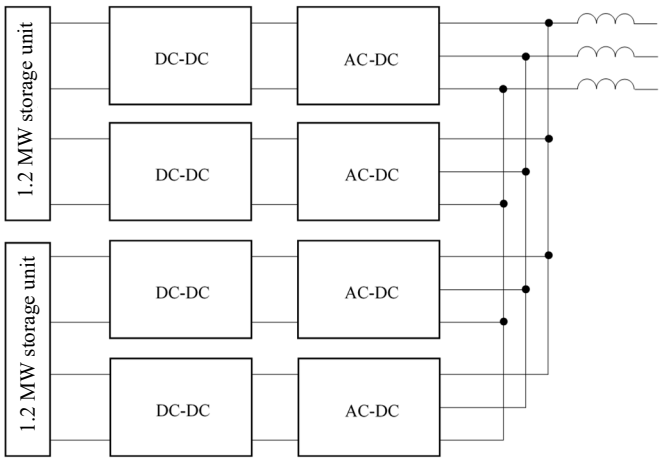

Fig. 7 Flumeri (Italy) Sodium-Sulphur storage installation scheme

However, an improvement of the performed simulations could be performed by carrying out a measurement campaign on the NaS batteries and by inferring an experimental NaS battery model in Matlab Simulink, in accordance with other Na-beta experimental model [9-12]. In fig. 10 the DC bus voltage during the inversion simulation is shown, for a reference voltage U^*_{DC}=1050 V. It is possible to observe that the DC bus voltage control takes about 200 ms to stabilize the reference DC voltage value. The total harmonic distortion (THD) of the grid current calculated in this simulation is equal to 3.01% and the harmonic spectrum in p.u. with respect to the fundamental frequency is shown in detail in fig. 11. In order to verify the present control approach for continuously variable grid power requirements, the instantaneous model response has been tested for an imposed active power from 800 kW to -800 kW and an imposed reactive power from 500 kvar to -500 kvar.

The simulation results are shown in fig. 12. The DC bus voltage behaviour during this simulation is shown in fig. 13, where it is possible to see the effectiveness of the adopted DC-bus voltage control (reference voltage U^*_{DC}=1050 V).

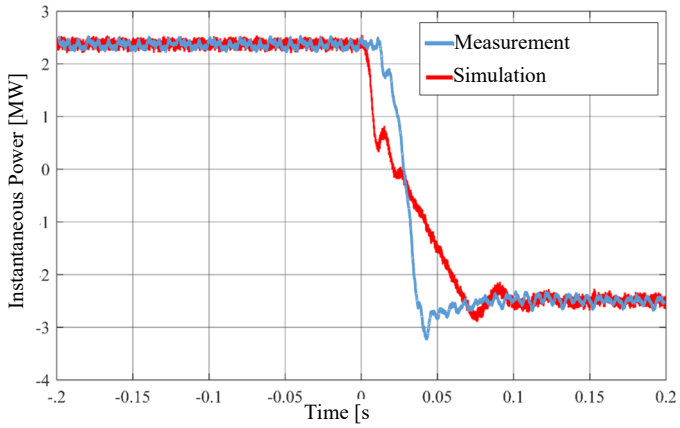

Fig. 8 Comparison between model results and experimental measurement. In the model the power variation time has been set equal to 10 ms

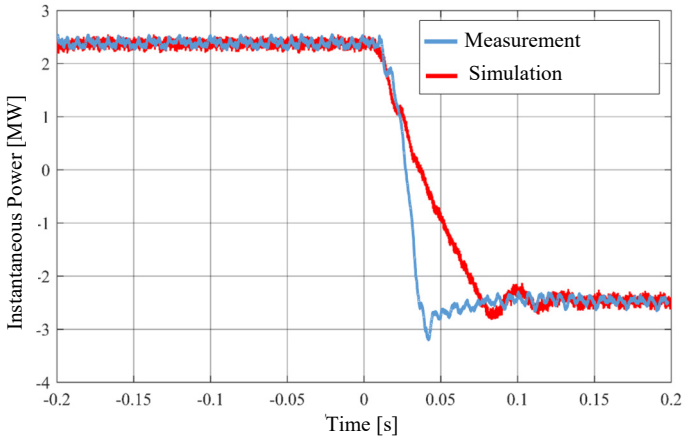

Fig. 9 Comparison between model results and experimental measurement. In the model the power variation time has been set equal to 30 ms

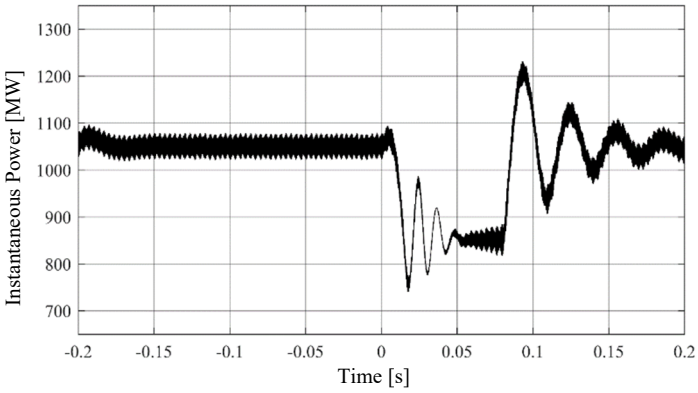

Fig. 10 DC bus voltage during the power inversion

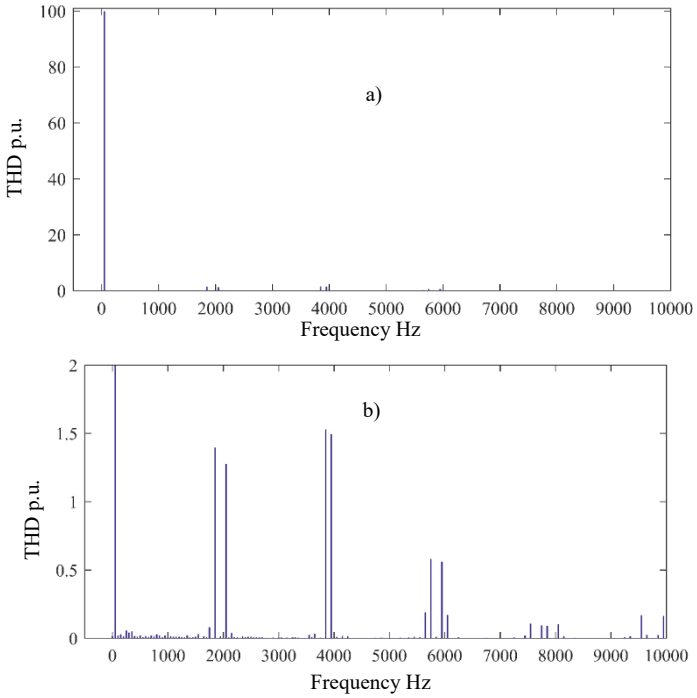

Fig. 11 a) THD of the grid current in p.u; b) zoom of the THD of the grid current in p.u.

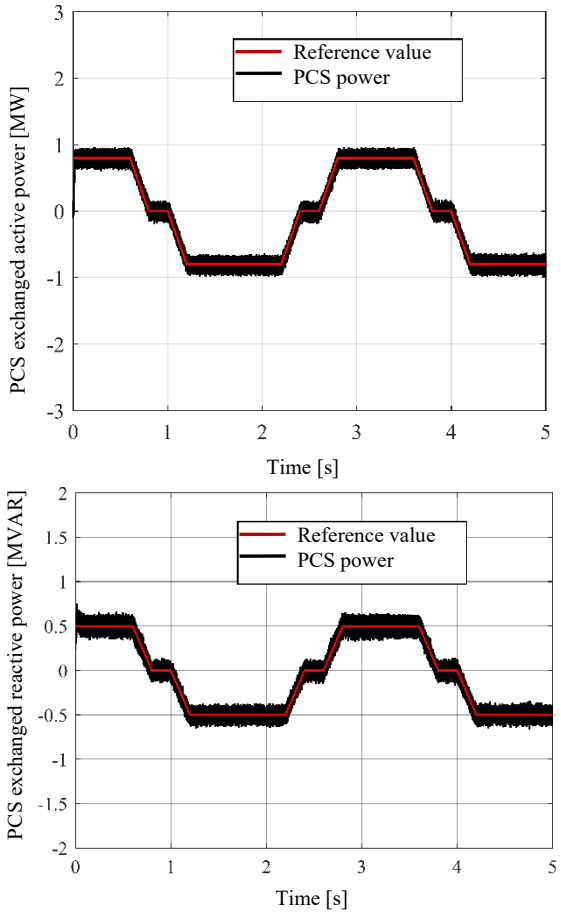

Fig. 12 PCS model simulation test: inverter supplied active power a) and reactive one b) vs the power reference values (red lines)

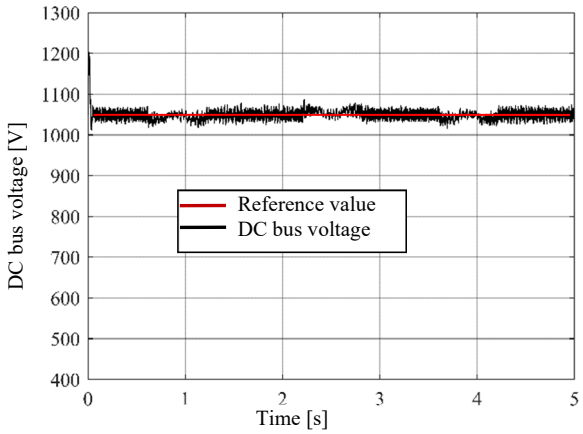

Fig. 13 DC bus voltage during the simulation of fig. 13

IV CONCLUSIONS

A PCS control scheme, suitable to interface an ESS with the HV network, has been applied to a two stage PCS Simulink model. The model results have been compared with experimental measurements performed by the Italian TSO Terna during an ESS power inversion. By taking into account the lack of data on the EES system, the agreement between model results and measurements is satisfactory. In fact, the main differences between measurements and model results can be imputed to ESS dynamic during the phase inversion. The simulations show that promptness of the present PCS control, which allows having inversion times lower than 100 ms, is in tune with the Italian network requirements and the current THD is fully acceptable. Moreover, simulations have been performed to verify the PCS model instantaneous response for variable active and reactive power reference values. The power supplied by the converter follows very well the power reference values.

REFERENCES

[1] M. Andriollo, R. Benato, M. Bressan, S. Dambone Sessa, F. Palone, R. M. Polito: Review of Power Conversion and Conditioning Systems for Stationary Electrochemical Storage, *Energies* 2015, 8(2), 960-975; doi:10.3390/en8020960

[2] R. Benato, N. Cosciani, G. Crugnola, S. Dambone Sessa, G. Lodi, C. Parmeggiani, M. Todeschini: “Sodium nickel chloride battery technology for large-scale stationary storage in the high voltage network”, *J. of Power Sources*, 293 (2015) 127–136, doi:http://dx.doi.org/10.1016/j.jpowsour.2015.05.037.

[3] R. Teodoreschu, M. Liserre, P. Rodriguez: “Grid Converters For Photovoltaic and Wind Power Systems”, 2011 John Wiley & Sons, Ltd. ISBN: 978-0-470-05751-3

[4] Park, R. H., ‘Two Reaction Theory of Synchronous Machines. Generalized Method of Analysis – Part I’. In *Proceedings of the Winter Convention of the AIEE*, 1929, pp. 716–730.

[5] Clarke, E., Circuit Analysis of AC Power Systems, Vol. 1, New York: John Wiley & Sons, Inc., 1950.

[6] Bito A.: "Overview of the sodium-sulfur battery for the IEEEStationary Battery Committee". *IEEE Power Engineering Society General Meeting*, Vol. 2, 2005, p. 1232-1235.

[7] Tamakoshi T.: "Recent sodium sulfur battery applications inJapan", *ESA 2001 Annual Meeting in Chattanooga*, Tennessee, April 26-27, 2001.

[8] M. Andriollo, R. Benato, S. Dambone Sessa, N. Di Pietro, N. Hiray, Y. Nakanishi, E. Senatore: “Energy intensive electrochemical storage in Italy: 34.8 MW sodium-sulphur secondary cells”, *Journal of Energy Storage*, Vol. 5, Pag. 146-155, 2016.

[9] S. Dambone Sessa, G. Crugnola, M. Todeschini, S. Zin, R. Benato: "Sodium nickel chloride battery steady-state regime model for stationary electrical energy storage", *Journal of Energy Storage*, 6, pp. 105-115, 2016.

[10] S. Dambone Sessa, F. Palone, A. Necci, R. Benato: "Sodium-nickel chloride battery experimental transient modelling for energy stationary storage*", Journal of Energy Storage*, Vol. 9, pp. 40-46, 2017.

[11] T.M. O'sullivan, C.M. Bingham, R.E. Clark, Zebra battery technologies for the all electric smart car, SPEEDAM International Symposium on Power Electronics, Electrical Drives, Automation and Motion (2006).

[12] M. Sudoh, J. Newman, Mathematical modeling of the sodium/iron chloride battery, J. Electrochem. Soc. 137 (3) (1990) 876–883, doi:http://dx.doi.org/10.1149/1.2086571.